

## Lehigh University Lehigh Preserve

---

Fritz Laboratory Reports

Civil and Environmental Engineering

---

1969

# Significance and application of stub column test results, June 1969 (71-18)

C. K. Yu

L. Tall

Follow this and additional works at: <http://preserve.lehigh.edu/engr-civil-environmental-fritz-lab-reports>

---

### Recommended Citation

Yu, C. K. and Tall, L., "Significance and application of stub column test results, June 1969 (71-18)" (1969). *Fritz Laboratory Reports*. Paper 1838.  
<http://preserve.lehigh.edu/engr-civil-environmental-fritz-lab-reports/1838>

This Technical Report is brought to you for free and open access by the Civil and Environmental Engineering at Lehigh Preserve. It has been accepted for inclusion in Fritz Laboratory Reports by an authorized administrator of Lehigh Preserve. For more information, please contact [preserve@lehigh.edu](mailto:preserve@lehigh.edu).

Welded Built-Up and Rolled Heat-Treated T-1 Steel Columns

SIGNIFICANCE AND APPLICATION OF STUB COLUMN TEST RESULTS

by

C. K. Yu and L. Tall

This work has been carried out as part of an investigation sponsored by the United States Steel Corporation. Technical guidance was provided by the Task Group 1 of the Column Research Council.

Fritz Engineering Laboratory  
Department of Civil Engineering  
Lehigh University  
Bethlehem, Pennsylvania

June, 1969

Fritz Laboratory Report No. 290.18

TABLE OF CONTENTS

	<u>Page</u>
ABSTRACT	
1. INTRODUCTION	1
2. BASIC CONCEPTS	3
3. EFFECTIVE TANGENT MODULUS VS. EFFECTIVE MOMENT OF INERTIA RELATIONSHIPS	9
4. APPLICATION OF STUB COLUMN TEST RESULTS	17
5. SUMMARY AND CONCLUSIONS	20
6. ACKNOWLEDGEMENTS	23
7. NOMENCLATURE AND DEFINITIONS	24
8. APPENDIX	26
9. FIGURES	30
10. REFERENCES	46

ABSTRACT

The basic relationship is established between the stress-strain curve obtained from a stub column test and the basic column strength curve. Charts are prepared to allow the prediction of the buckling load of steel columns from stub column results. This approach simplifies the process of predicting column strength and eliminates full-scale column tests and the measurement of residual stresses.

## 1. INTRODUCTION

Two approaches can be taken for the computation of the tangent modulus flexural buckling load of columns. One is based on the measured or assumed residual stress pattern and the stress-strain relationship, employing a numerical procedure or an analytical method; the other is based on stub column test results and is a semi-empirical method. The first approach has been subjected to extensive investigation. (1 through 4) However, the method itself is complicated in general and usually needs experimental verification by full scale column tests, except for a few simple cases. The second approach is simpler, more economical and gives solutions closer to the actual behavior of columns. The second approach is discussed in this report.

A stub column is defined as a column long enough to retain the original magnitude of residual stresses in the section and short enough to prevent any premature column failure from occurring before the yield load of the section is obtained. (5) A stub column test is performed in order to obtain an average stress-strain curve for the complete cross section which takes into account the effects of residual stresses.

The application of stub column test results to the prediction of column strength has been developed and used

widely during the past decade. However, the method has been applied mostly for rolled shapes made of steel with an elastic perfectly-plastic stress-strain relationship.

Therefore, all the relevant relationships between the stress-strain curve obtained from a stub column test and the basic column strength were established for rolled shapes of mild steel only.

This study is to extend the previous research into shapes which have residual stresses of this welded type and/or are made of material which does not have an elastic perfectly-plastic stress-strain relationship.

## 2. BASIC CONCEPTS

Figure 1 illustrates diagrammatically the stress-strain curve of a material and the stub column curve (average stress-strain curve of the whole cross section obtained from a stub column test). The slopes of the stress-strain curve and the stub column curve are referred to as tangent modulus,  $E_t$  and effective tangent modulus  $E_m$ , respectively. In the elastic range, both  $E_t$  and  $E_m$  are the modulus of elasticity,  $E$ . The stress at the proportional limit of the stress-strain curve is  $\sigma_p$ , whereas that of the stub column curve is  $\sigma_{pm}$ .

From a stub column test, the relationship between effective tangent modulus and the tangent modulus can be expressed as

$$E_m = \frac{d\sigma_{ave}}{d\varepsilon} = \frac{dP/A}{dP / \int_A E_t dA} = \frac{\int_A E_t dA}{A} \quad (1)$$

where,  $d\sigma_{ave}$  = the average stress increment,  $d\varepsilon$  = the corresponding strain increment,  $dP$  = increment of axial force, and  $A$  = the total cross-sectional area. If the effective area is defined as

$$A_m = \frac{E_t}{E} dA \quad (2)$$

where  $A_m$  can be considered as an equivalent elastic section that functions in a manner identical to the actual section in which part or all of the section is in the inelastic range, as far as column buckling strength is concerned, then, from Eqs. 1 and 2,

$$\frac{E_m}{E} = \frac{A_m}{A} \quad (3)$$

For a centrally loaded column, the critical load,  $P_{cr}$ , based on the tangent modulus concept is (6)

$$P_{cr} = \frac{\pi^2 E \int_A \frac{E_t}{E} y^2 dA}{L^2} \quad (4)$$

Comparing the term  $\int_A \frac{E_t}{E} y^2 dA$  which is defined as the effective moment of inertia  $I_m$ , with the expression in Eq. 2, then,  $I_m$  is simply the moment of inertia of the effective area. Consequently

$$I_m = f\left(\frac{A_m}{A}\right) = f\left(\frac{E_m}{E}\right)$$

where the  $f$  function is dependent on the shape of the effective area. The critical load can be expressed simply



as

$$P_{cr} = \frac{\pi^2 EI_m}{L^2} \quad (5)$$

or, in a nondimensional form

$$\lambda = \frac{1}{\pi} \sqrt{\frac{\sigma_y}{E}} \cdot \frac{L}{r} = \sqrt{\frac{I_m/I}{P_{cr}/P_y}} \quad (6)$$

To apply the results of the stub column test to the prediction of the column buckling load, the relationship between  $\frac{E_m}{E}$  obtained from the stub column test and the corresponding  $\frac{I_m}{I}$ , or the shape of effective area, needs to be known beforehand. For simple cross sections such as a rectangle, or a circular tube, which also has a residual stress pattern of cooling after rolling and exhibits an elastic perfectly-plastic stress-strain behavior, constant relationship between  $E_m$  and  $I_m$  can be established, since the shape of  $A_m$  remains the same throughout the complete loading process. However, for more complicated sections, or for shapes which do not have the rolling type residual stresses in the cross section and/or do not follow the elastic-perfectly-plastic stress-strain law, the relationship between  $I_m$  and  $E_m$  could be very much involved and usually is a function of not only the cross-sectional properties but also of the stress-strain curve

and of both the magnitude and pattern of the residual stress distribution.

To illustrate this point, an example is given here for a rectangular section with a triangular type residual stress distribution and a stress-strain curve represented by two straight lines connected by a parabolic transition curve as shown in Fig. 2. Only one-dimensional residual stresses, that is, no variation of residual stress across the thickness,  $t$ , are considered, and the principal axis which is parallel to the direction along which residual stress varies is designated as the  $x$ -axis and the other axis as the  $y$ -axis. For bending about the  $x$ -axis, the modified moment of inertia,  $I_{mx}$ , can be expressed as

$$I_{mx} = \int_A \frac{E_t}{E} y^2 dA = \int_{A_m} y^2 dA_m \quad (7)$$

where

$$dA_m = \left( \frac{E_t}{E} \cdot dx \right) \cdot t = d \cdot d\bar{x}$$

Since only the width of a differential element is changed after loading, the shape of the effective section will remain as a rectangle. Therefore the relationship between  $E_m$  and  $I_{mx}$  is simply

$$\frac{I_{mx}}{I_x} = \frac{E_m}{E} \quad (8)$$

This expression is true even for a stress-strain curve and for a residual stress pattern other than those described in this example.

However, for buckling with respect to the y-axis (Fig. 2c), the modified moment of inertia,  $I_{my}$ , is

$$I_{my} = \int_A \frac{E_t}{E} x^2 dA = \int_{A_m} x^2 dA_m \quad (9)$$

where  $dA_m = \frac{E_t}{E} \cdot t \cdot dx = \bar{t} dx$ . In this case the width of a differential element of the area of the effective section depends on its distance,  $x$ , from the y-axis, and therefore the shape of the effective section could vary from load to load as shown in Fig. 2c. In this example, because the assumed  $E_t$  vs.  $\epsilon$  relationship is linear in the inelastic range, the effective areas are bounded by straight lines. The explicit expressions of  $I_{my}/I_y$  vs.  $E_m/E$  are given in the Appendix.

For most practical sections such as wide flange shapes, the explicit exact relationship between  $I_m/I$  and  $E_m/E$  is more complicated and sometimes impossible to derive especially for shapes made of non-linear materials. It is proposed here that the  $I_m/I$  vs.  $E_m/I$  relationship for complex cases should be presented in the form of charts. A numerical procedure is adopted to compute the exact solutions. The

numerical computation is accomplished as follows:

1. Divide the section into a sufficient number of finite area elements as shown in Fig. 3.
2. Record the residual strain at the center of each element assuming that the residual stresses distributed over each element are uniform with the magnitude the same as that at the center.
3. Apply a uniform strain larger than the difference between yield strain and maximum compression residual strain on the cross section. The total strain at an element is equal to the residual strain plus the applied uniform longitudinal strain.
4. From the tangent modulus strain equation, determine the tangent modulus corresponding to the total strain computed in step 3 for each element.
5. Compute,  $E_m = \sum_{i=1}^N (E_t)_i \cdot \Delta A$  and  $I_m = \sum_{i=1}^N (E_t)_i \cdot y_i^2 \cdot \Delta A$  where  $N$  is the total number of finite area elements into which the section is divided.
6. Increase the applied uniform longitudinal strain and repeat steps 1 through 5 until the entire cross-section is yielded or strain-hardened.

### 3. EFFECTIVE TANGENT MODULUS VS. EFFECTIVE MOMENT OF INERTIA RELATIONSHIPS

The effective tangent modulus vs. effective moment of inertia relationship for rolled wide flange sections and for welded H-shapes are discussed. Two kinds of stress-strain relationships, the elastic perfectly-plastic and the nonlinear (such as that of A514 steel), are considered. For the complex cases, the  $E_m$  vs.  $I_m$  relationships are presented in charts.

#### Shapes with an Elastic Perfectly-Plastic Stress-Strain Curve:-

For material having an elastic perfectly-plastic stress-strain relationship, the tangent modulus  $E_t$  must be either equal to  $E$  or zero. Therefore, from Eqs. 2 and 3, for a given section with residual stress,  $A_m = A_e$  and  $\frac{E_m}{E} = \frac{A_e}{A}$  where  $A_e$  is the remaining unyielded area, or elastic area. The effective moment of inertia simply is the moment of inertia of the elastic area,  $I_e$ .

For small and medium-size rolled shapes made of mild steel, the stress-strain curve of the material and the patterns of residual stress distributions can be represented as shown in Fig. 4. If the web of the wide flange is neglected, the effective area, or elastic

area in this case, will remain as two separated identical rectangles parallel to each other. Then

$$\frac{I_{mx}}{I_x} = \frac{A_e}{A} = \frac{E_m}{E} \quad (10)$$

and

$$\frac{I_{my}}{I_y} = \frac{A_e^3}{A^3} = \frac{E_m^3}{E^3} \quad (11)$$

These approximate solutions were first presented by Huber and Beedle.<sup>(7)</sup> However, it would be interesting to examine the effect of the web area which is neglected in Eqs. 10 and 11. Four sections, namely, 8WF31, 12WF40, 10WF49 and 14WF426, which represent typical column sections are selected for illustration. The relationship between  $E_m$  and  $I_m$  is presented in chart form with  $E_m/E$  as ordinate and  $I_m/I$  abscissa. Figure 5 shows the exact solutions considering the web area, bending with respect to strong axis, and Eq. 10 is represented by a straight line of 45 degrees. Compare the exact solutions for the four representative section with the approximate solution; it indicates that the maximum difference is approximately 4% of that obtained from Eq. 10, and the  $E_m/E$  vs.  $I_{mx}/I_x$  relationship is independent of the magnitude of residual stress. Therefore, Eq. 10 may be applicable to all the

wide flange shapes, if a maximum error of 4% can be considered acceptable.

For weak axis bending, the  $E_m/E$  vs.  $I_{my}/I_y$  relationships for all four shapes coincide with the line which represents Eq. 11, as shown in Fig. 6. This indicates that the web area has practically no effect on  $I_{my}$ , and Eq. 11 can be considered as the exact solution for columns of rolled wide flange shapes, buckled with respect to the weak axis.

In Fig. 4, the penetration of yielding on the cross section is shown. When the load is applied, as long as the residual stress distribution causes yielding to be initiated at the flange tips and web center and gradually move towards the junctures of flange and web, that is, the patterns of residual stress is such that the maximum compressive residual stress is at flange tip and web center and the residual stress magnitude decreases toward the junctures of flanges and web, then Eqs. 10 and 11 are always applicable.

Welded H-shapes built-up from mild steel plates with the preparation of the plate edges as flame-cut or universal mill, may have residual stress patterns considerably different from those of rolled shapes.

Figure 7 shows the typical residual stress patterns in welded H-shapes; one with universal mill plates and the other with flame-cut plates.

It is apparent that when the external load is applied the partially yielded cross section of welded shapes with universal mill plate is the same as that of rolled shapes, as shown in Fig. 4. Hence, Eqs. 10 and 11 are still applicable for welded columns built-up from universal mill plates.

However, for welded H-shapes with flame-cut plates, the residual stress distribution is somewhat different from those aforementioned. Due to the flame-cutting process, a tensile residual stress of approximately 75% of the yield stress exists at the flange tips, and due to the welding, a tensile residual stress approximately equal to the yield stress exists at the juncture of flange and web. The compressive residual stress is nearly constant and distributed over the flanges away from the center and edges, and on the web near its center portion, as shown in Fig. 7. The magnitude of compressive residual stress is in general inversely proportional to the width-thickness ratio of the component plate. For strong axis buckling, the exact  $E_m/E$  vs.  $I_{mx}/I_x$  relationships for four columns sections are shown in Fig. 8. It is observed that the curves are very close to those obtained for rolled shapes.



Apparently, the shifting of the location of the remaining elastic area on the flanges in the x-axis direction, caused by the tensile residual stress at flange tips, does not change the  $E_m/E$  vs.  $I_{mx}/I_x$  relationship. Equation 10 therefore, can be extended to cover welded H-shapes with flame cut plates.

For the weak axis bending, because of the tensile residual stress at flange tips, welded H-shapes built-up from flame-cut plates behave considerably different from rolled shapes or welded shapes with UM plates. The  $E_m/E$  vs.  $I_{my}/I_y$  relationship for a 12H40 is shown in Fig. 9. The magnitude of compressive residual stresses used in Fig. 9 varies from  $0.2\sigma_y$  to  $0.88\sigma_y$ . It is observed that the exact solutions are far removed from the solution given by Eq. 11 and, in addition, the  $E_m/E$  vs.  $I_{my}/I_y$  relationships are dependent on the magnitude of the compressive residual stress. However, the differences among the curves are not significant.

The effect of sectional properties was also investigated for four different column sections, and it was found that the dimensions of the section do not change the shape of the curve. Figure 10 shows the curves for  $\sigma_{rc}$  equal to  $0.88\sigma_y$ .

In Fig. 9, it is observed that the differences among the five curves, representing  $\sigma_{rc}$  varying from  $0.2\sigma_y$  to  $0.88\sigma_y$ , are insignificant. The curve for  $\sigma_{rc}$  equal to  $0.88\sigma_y$  (extreme case for this pattern of residual stress) gives the most conservative prediction of column strength. This curve, which is shown in Fig. 10, should be used to represent the  $E_m/E$  vs.  $I_{my}/I_y$  relationship for all the welded shapes with flame-cut plates.

Shapes with a Nonlinear Stress-Strain Curve: -

For the purposes of this study, A514 steel was considered.

A514 steel has a nonlinear stress-strain relationship which consists of an elastic range, a transition range, and a strain-hardening range. The stress-strain curve can be described by the following three equations<sup>(6)</sup>

$$\frac{\sigma}{\sigma_y} = \frac{\epsilon}{\epsilon_y} \quad \text{when} \quad 0 \leq \frac{\sigma}{\sigma_y} \leq 0.8 \quad (12)$$

$$\begin{aligned} \frac{\sigma}{\sigma_y} = & 1.0 + 0.005 \left( \frac{\epsilon}{\epsilon_y} - 1.517 \right) + 0.3647 \left( \frac{\epsilon}{\epsilon_y} - 1.517 \right)^3 \\ & + 0.3276 \left( \frac{\epsilon}{\epsilon_y} - 1.517 \right)^5 \end{aligned}$$

$$\text{when} \quad 0.8 \leq \frac{\sigma}{\sigma_y} \leq 1.0 \quad (13)$$

and 
$$\frac{\sigma}{\sigma_y} = 1.0 + 0.005 \left( \frac{\epsilon}{\epsilon_y} - 1.517 \right)$$

when 
$$\frac{\sigma}{\sigma_y} < 1.0 \quad (14)$$

where  $\sigma$  = stress,  $\sigma_y$  = yield stress determined by the 0.2% offset method,<sup>(8)</sup>  $\epsilon$  = strain, and  $\sigma_y = \text{yield strain} (= \sigma_y/E)$ . Figure 11 shows the complete stress-strain curve for A514 steel.<sup>(6)</sup> Due to the nonlinearity of the stress-strain curve, it was found that, contrary to the case of sections with an elastic perfectly-plastic stress-strain curve, the magnitude of compressive residual stress has a pronounced influence on the  $E_m/E$  vs.  $I_{my}/I_y$  relationship. However, for strong axis bending, Eq. 10 is still valid, as mentioned above. Since the sectional properties have no significant influence,<sup>(7)</sup>  $E_m/E$  vs.  $I_{my}/I_y$  relationships are obtained for an H-shaped section having dimensions corresponding to an 8WF31 shape, and the results should be applicable to H-shapes of other dimensions as well.

Three types of residual stress distribution are considered, which represent possible patterns of residual stress in rolled shapes and in welded shapes with sheared-edge plates and with flame-cut plates. The  $E_m/E$  vs.  $I_{my}/I_y$

relationships are presented in the form of charts as shown in Fig. 12 to Fig. 14. In these figures, it is apparent that the magnitude of compressive residual stress could alter the shape of the curve considerably.

#### 4. APPLICATION OF STUB COLUMN TEST RESULTS

The application of the stub column test results and of the  $E_m/E$  vs.  $I_m/I$  relationship for the determination of column strength is described:

1. The approximate pattern of residual stress distribution in the cross section and the stress-strain relationship of the material must be known; then, the corresponding chart can be selected.
2. The effective tangent moduli are determined by drawing lines tangent to the stub column stress-strain relationship at different values of  $P/P_y$ ; the slopes of these lines define the corresponding effective tangent moduli.
3. To determine the maximum compressive residual stress,  $\sigma_{rc}$ , the proportional limit stress,  $\sigma_{pm}$ , of the stub column stress-strain curve must be first determined. This can be accomplished by locating the point on the stub column stress-strain curve where the slope starts to deviate from that of the modulus of elasticity,  $E$ . Then,  $\sigma_{rc}$  is simply equal to the difference between  $\sigma_p$  (stress at the

proportional limit on the stress-strain curve of the material) and  $\sigma_{pm}$ . That is,

$$\sigma_{rc} = \sigma_p - \sigma_{pm} \quad (15)$$

4. Based on the  $\sigma_{rc}$  determined, the corresponding chart and the exact or interpolated curve for  $\sigma_{rc}$  are used. The corresponding  $\frac{I_m}{I}$  for each measured  $\frac{E_m}{E}$  can then be determined.

5. The corresponding slenderness function,  $\lambda$ , for a set of  $\frac{P}{P_y}$ ,  $\frac{E_m}{E}$ , and  $\frac{I_m}{I}$  can be obtained from

$$\lambda = \frac{\sqrt{\frac{I_m}{I}}}{\frac{P}{P_y}} = \sqrt{\frac{\frac{E_m}{E}}{\frac{P}{P_y}}} \quad (16)$$

*for bending about weak axis (p. 15)*

6. The slenderness function,  $\lambda$ , is calculated at different  $P/P_y$  levels and the  $P/P_y$  vs.  $\lambda$  curve plotted; this is the column curve based on the stub column test results.

The results of tests of two stub columns, one welded 7H28 shape with sheared edge plates and the other a welded 7H28 shape with flame-cut plates, both of A514 steel, are selected here as an example. The load-strain curves

of the stub columns are shown in Fig. 15a. The column curves based on these two stub column tests are shown in Fig. 15b. Column curves based on the measured residual stresses obtained by means of a numerical analysis are also presented in Fig. 15b. The comparison of column curves obtained by these two different approaches shows that good correlation exists between them. The small difference can be accounted for in the error induced in the determination of the effective modulus; also the actual residual stress distribution in the section could be slightly different from that assumed in the development of the  $E_m/E$  vs.  $I_m/I$  curves. The column test points are also shown on the same figure (Fig. 15b) to give some indications of the accuracy of the theoretical curves.

The advantage of using stub column tests to predict the column strength is that, if the stub column test is conducted carefully, there is no need to perform full size column tests and residual stress measurements. As long as the related  $\frac{E_m}{E}$  vs.  $\frac{I_m}{I}$  relationship is available, column strength can be predicted rather accurately from the results of stub column tests.

## 5. SUMMARY AND CONCLUSIONS

The basic relationship between the stress-strain curve obtained from a stub column test and the basic column strength curve is established.

These relationships are given by

$$P_{cr} = \frac{\pi^2 EI_m}{L^2} \quad (5)$$

$$\frac{I_{mx}}{I_x} = \frac{A_e}{A} = \frac{E_m}{E} \quad (10)$$

$$\frac{I_{my}}{I_y} = \frac{A_e^3}{A} = \frac{E_m^3}{E} \quad (11)$$

where  $P_{cr}$  = tangent modulus buckling load  
 $I_m$  = effective moment of inertia  
 $A_e$  = area remaining elastic  
 $E_m$  = effective tangent modulus  
 (tangent modulus from stub column test)

Charts are prepared to accommodate the prediction from stub column test results of the tangent modulus buckling load of columns made of either mild steel or A514 steel, welded or rolled shapes. This approach simplifies the process of prediction of column strength and eliminates the necessities of full-scale column tests and residual stress measurement. The following conclusions



may be drawn from this study:

1. The approximate relationship (Eqs. 10 and 11) between the effective tangent modulus (obtained from a stub column test) and the elastic moment of inertia is valid for shapes which have an elastic-perfectly-plastic stress-strain curve and have the maximum compressive residual stress at the flange tips with decreasing values towards the center of the flange. For other shapes, the relationship between the average tangent modulus and the "effective moment of inertia" with respect to the weak axis is very involved and must be treated individually.
2. For strong axis buckling of H-shapes, the relationship between the effective tangent modulus and the effective moment of inertia is practically linear irrespective of the stress-strain relationship and the pattern of residual stresses.
3. For weak axis buckling, Eq. 11 is applicable, for rolled shapes and welded shapes built up from universal mill plates made of steel which has an elastic-perfectly-plastic stress-strain

relationship. Each other case must be treated separately. A numerical method is employed to determine the relationship between the effective tangent modulus and the effect moment of inertia. The results are presented in the form of charts. Each of these charts represents a combination of a stress-strain relationship and a certain pattern of residual stress. By using these charts, the corresponding effective moment of inertia for a given effective tangent modulus can be easily determined.

4. The sectional properties of an H-shaped section do not affect the  $E_m/E$  vs.  $I_{my}/I_y$  relationship but do affect slightly the  $E_m/E$  vs.  $I_{mx}/I_x$  relationship; however, the difference is insignificant.

Column strength may be predicted accurately and directly from the stress-strain relationship of the stub column test.

## 6. ACKNOWLEDGEMENTS

The investigation was conducted at Fritz Engineering Laboratory, Department of Civil Engineering, Lehigh University, Bethlehem, Pennsylvania. The investigation was part of a major study into the strength of welded built-up and rolled heat-treated "T-1" steel columns.

The United States Steel Corporation sponsored the study, and appreciation is due to Charles G. Schilling of that company who provided much information and gave many valuable comments. Column Research Council Task Group I, under the chairmanship of John A. Gilligan, provided valuable guidance. Appreciation is due to Lynn S. Beedle, Director of Fritz Laboratory, who gave inspiration and advice throughout the study.

## 7. NOMENCLATURE AND DEFINITIONS

A	Area of cross section
$A_m$	Effective Area $( = \int \frac{E_t}{E} dA )$
b	Width of flange
-	
b	Effective width
d	Depth of section
e	Subscript denoting elastic
E	Modulus of elasticity
$E_m$	Effective tangent modulus, determined from stress-strain relationship of stub column test
$E_{st}$	Strain-hardening modulus
$E_t$	Tangent modulus
f	a function
I	Moment of Inertia - subscripts x and y refer to the x and y axes (strong and weak axes), respectively
$I_e$	Moment of inertia of elastic portion of cross section - subscripts x and y refer to the x and y axes, respectively
$I_m$	Effective moment of inertia $( = \int_A \frac{E_t}{E} y^2 dA )$ -subscripts x and y refer to the x and y axes, respectively.
L	Column length
m	Subscript denoting effective
P	Axial load

$P_{cr}$	Buckling load, or critical load; tangent modulus concept
$P_y$	Yield load in a column
$r$	Radius of gyration = subscripts x and y refer to strong and weak axis radii.
$t$	Thickness of flange
$u, v, w$	Displacement in the x, y, and z directions, respectively
$x, y, z$	Coordinate axes, coordinates of the point with respect to x, y, and z axes
$\epsilon$	Strain
$\epsilon_p$	Strain at proportional limit
$\epsilon_r$	Residual strain
$\epsilon_{rc}$	Maximum compressive residual strain
$\epsilon_{rt}$	Maximum tensile residual strain
$\epsilon_{st}$	Strain at start of strain hardening
$\epsilon_y$	Yield strain ( = $\sigma_y/E$ )
$\sigma$	Stress
$\sigma_{cr}$	Critical stress
$\sigma_p$	Stress at proportional limit
$\sigma_{pm}$	Proportional limit stress determined from a stub column test
$\sigma_r$	Residual stress
$\sigma_{rc}$	Maximum compressive residual stress
$\sigma_{rt}$	Maximum tensile residual stress
$\sigma_y$	Yield stress (determined by 0.2% offset method for non-linear stress-strain relationship)
$\Sigma$	Summation

8. APPENDIX

## APPENDIX:

EFFECTIVE MOMENT OF INERTIA AND EFFECTIVE  
TANGENT MODULUS RELATIONSHIP FOR A  
RECTANGULAR SECTION

1. Stress-Strain Relationship of the Material (Fig.2a):

$$\frac{\sigma}{\sigma_y} = \frac{\epsilon}{\epsilon_y} \quad \text{Elastic Range}$$

$$\frac{\sigma}{\sigma_y} = -\frac{1}{8} + \frac{3}{2} \left(\frac{\epsilon}{\epsilon_y}\right) - \frac{1}{2} \left(\frac{\epsilon}{\epsilon_y}\right)^2 \quad \text{Transition Range}$$

$$\frac{\sigma}{\sigma_y} = 1 \quad \text{Perfectly-Plastic Range}$$

2. Residual Stress Distribution (Fig.2b):

Triangular type with maximum compressive stress

$$\sigma_{rc} = 0.3\sigma_y.$$

3. Average Stress-Strain and Tangent Modulus-Strain

Equations (Stub Column Curves, Fig. 2a)

$$\text{when } 0 \leq \frac{\epsilon}{\epsilon_y} \leq 0.2$$

$$\frac{\sigma}{\sigma_y} = \frac{\epsilon}{\epsilon_y}$$

$$\frac{E_m}{E} = 1.0$$

when  $0.2 \leq \frac{\epsilon}{\epsilon_y} \leq 0.8$

$$\frac{\sigma}{\sigma_y} = -0.278 \left(\frac{\epsilon}{\epsilon_y}\right)^3 + 0.167 \left(\frac{\epsilon}{\epsilon_y}\right)^2 + 0.967 \left(\frac{\epsilon}{\epsilon_y}\right) + 0.0022$$

$$\frac{E_m}{E} = -0.833 \left(\frac{\epsilon}{\epsilon_y}\right)^2 + 0.333 \left(\frac{\epsilon}{\epsilon_y}\right) + 0.967$$

when  $0.8 \leq \frac{\epsilon}{\epsilon_y} \leq 1.2$

$$\frac{\sigma}{\sigma_y} = -0.5 \left(\frac{\epsilon}{\epsilon_y}\right)^2 + 1.5 \left(\frac{\epsilon}{\epsilon_y}\right) - 0.14$$

$$\frac{E_m}{E} = -\left(\frac{\epsilon}{\epsilon_y}\right) + 1.5$$

when  $1.2 \leq \frac{\epsilon}{\epsilon_y} \leq 1.8$

$$\frac{\sigma}{\sigma_y} = 0.139 \left(\frac{\epsilon}{\epsilon_y}\right)^3 - 0.75 \left(\frac{\epsilon}{\epsilon_y}\right)^2 + 1.35 \left(\frac{\epsilon}{\epsilon_y}\right) - 0.31$$

$$\frac{E_m}{E} = 0.417 \left(\frac{\epsilon}{\epsilon_y}\right)^2 - 1.5 \left(\frac{\epsilon}{\epsilon_y}\right) + 1.35$$

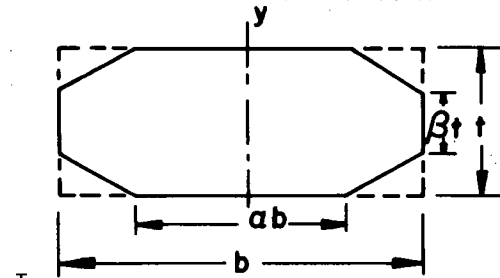
and when  $1.8 \leq \frac{\epsilon}{\epsilon_y}$

$$\frac{\sigma}{\sigma_y} = 1.0$$

$$\frac{E_m}{E} = 0.0$$



4.  $\frac{I_m}{I}$  vs.  $\frac{E_m}{E}$  Relationship (y-axis bending, Fig. 3.17c)



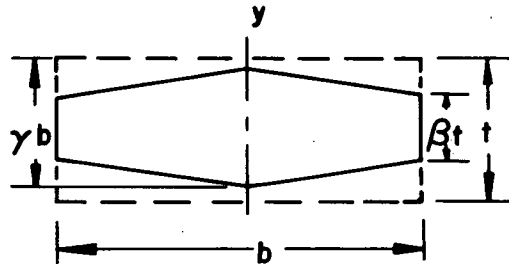
Elastic-Inelastic  
Range

$$(0.2 \leq \frac{\epsilon}{\epsilon_y} \leq 0.8)$$

$$\frac{I_m}{I} = 1 - \frac{1}{4} (1 - \alpha) (1 - \beta) (\alpha^2 + 2\alpha + 3)$$

$$= 1 - \sqrt{\frac{10}{3}} \left(1 - \frac{E_m}{E}\right)$$

$$= 0.2 \cdot (2 + 3\alpha)$$



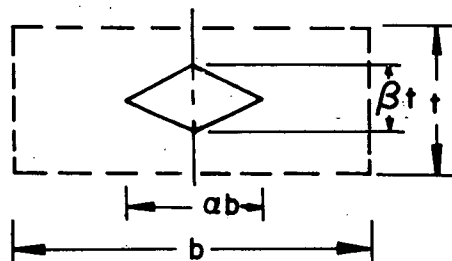
Inelastic Range

$$(0.8 \leq \frac{\epsilon}{\epsilon_y} \leq 1.2)$$

$$\frac{I_m}{I} = \frac{1}{4} (3\beta + \delta)$$

$$\delta = 0.3 + \frac{E_m}{E}$$

$$\beta = -0.3 + \frac{E_m}{E}$$



Inelastic Range

$$(1.2 \leq \frac{\epsilon}{\epsilon_y} \leq 1.8)$$

$$\frac{I_m}{I} = \frac{1}{4} \beta \alpha^3$$

$$\alpha = \frac{10}{3} \frac{E_m}{E}$$

$$\beta = 0.6\alpha$$

9. FIGURES

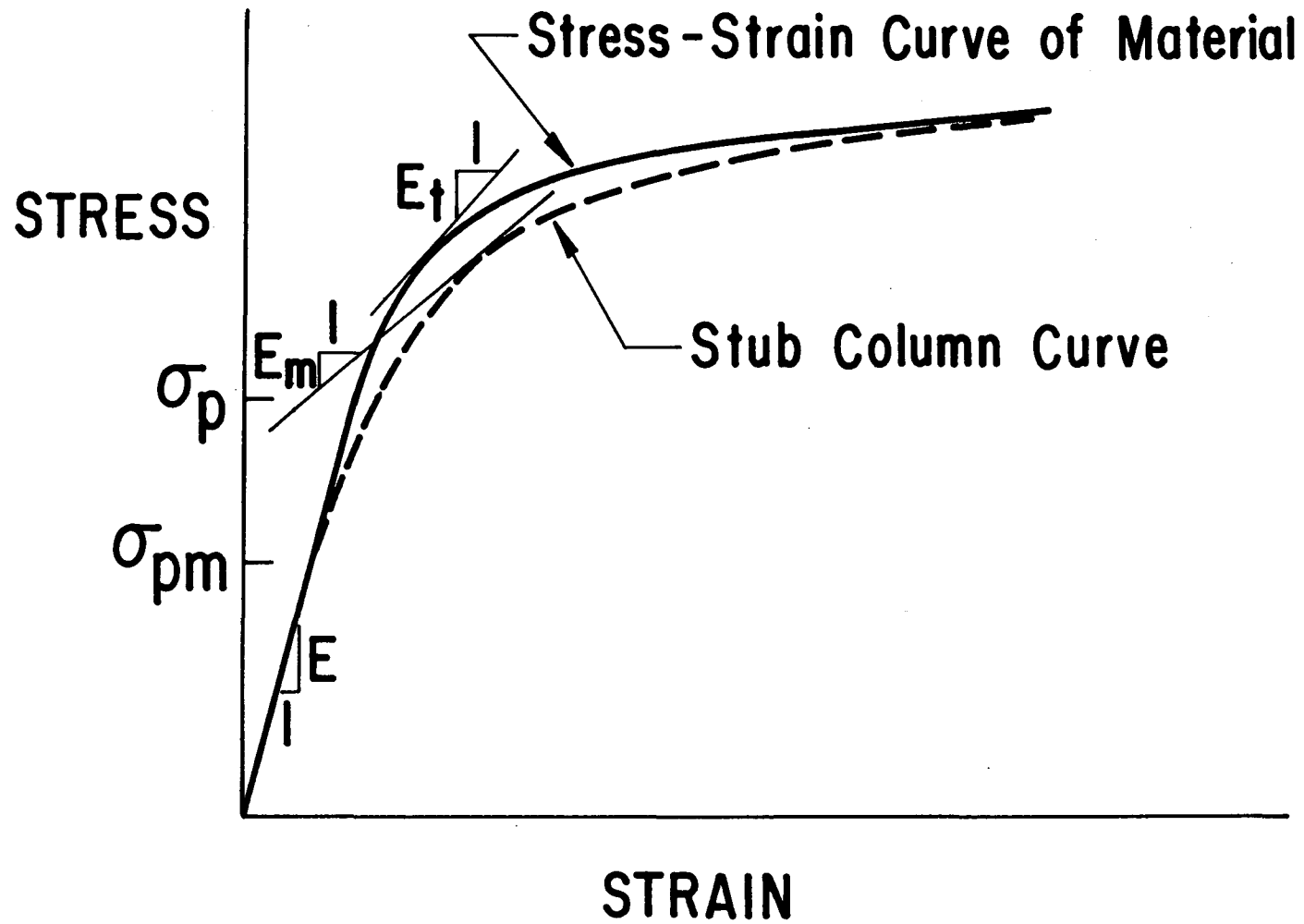


Fig. 1 Stress-Strain Curve and Stub Column Curve.

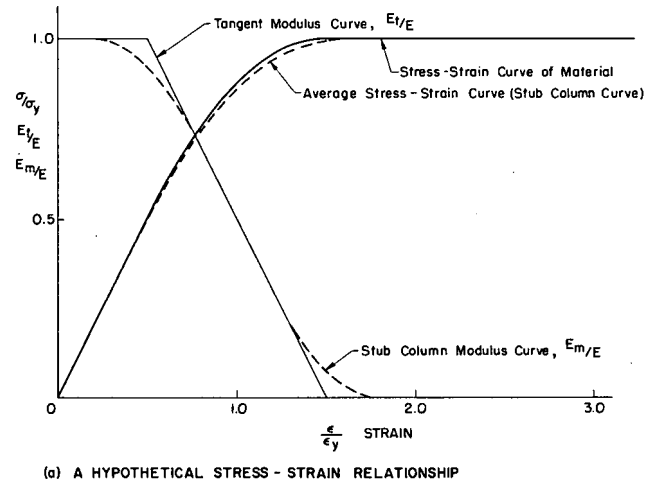
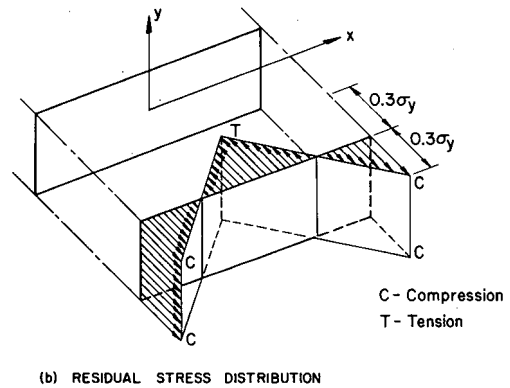
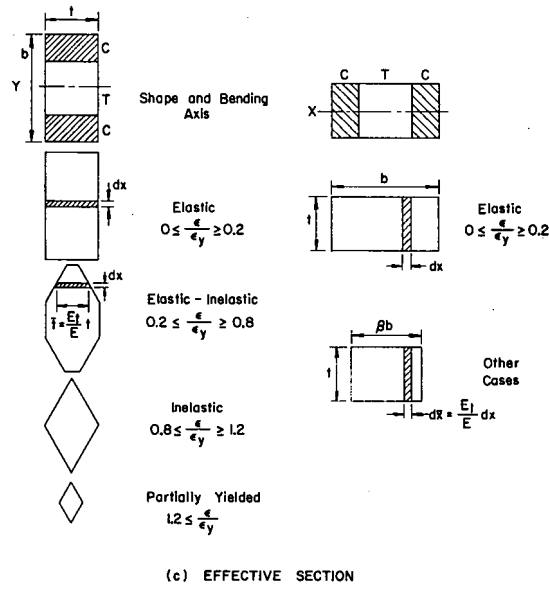


Fig. 2 Progress of the Effective Area for a Rectangular Section.

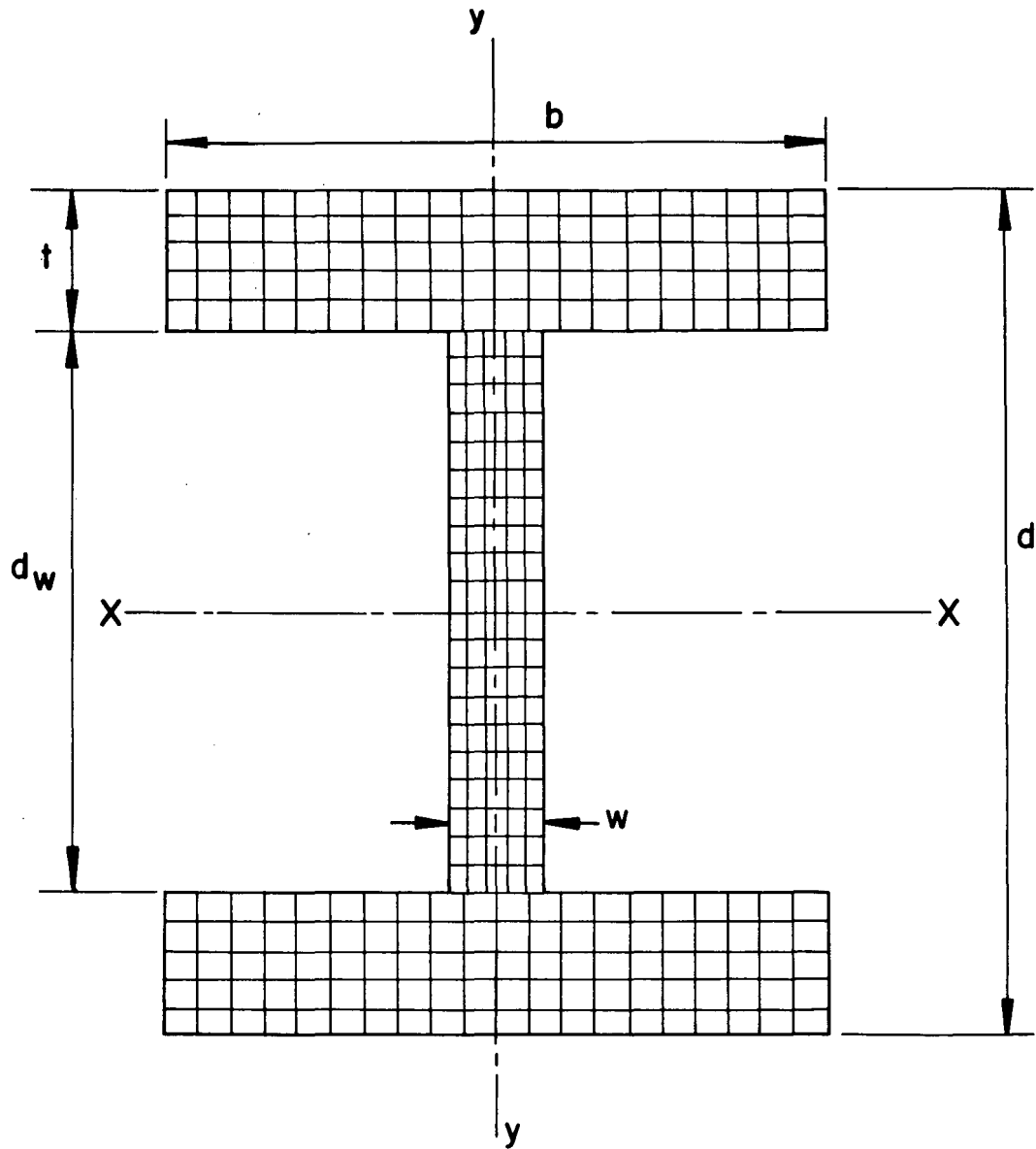
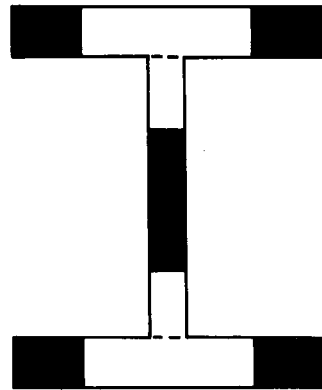
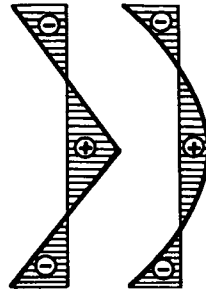
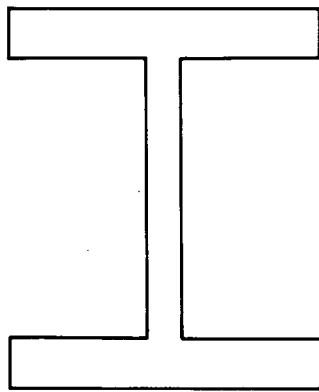
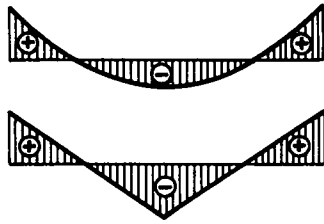
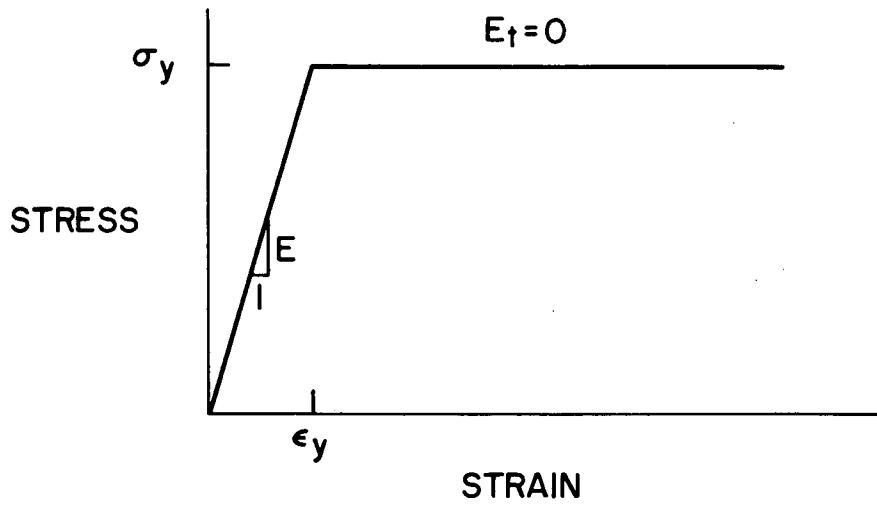


Fig. 3 Arrangement of Finite Area Elements.



RESIDUAL STRESS

PARTIALLY YIELDED CROSS-SECTION



STRESS STRAIN CURVE

Fig. 4 Residual Stress and Stress-Strain Curve for WF-Shapes of Mild Steels.

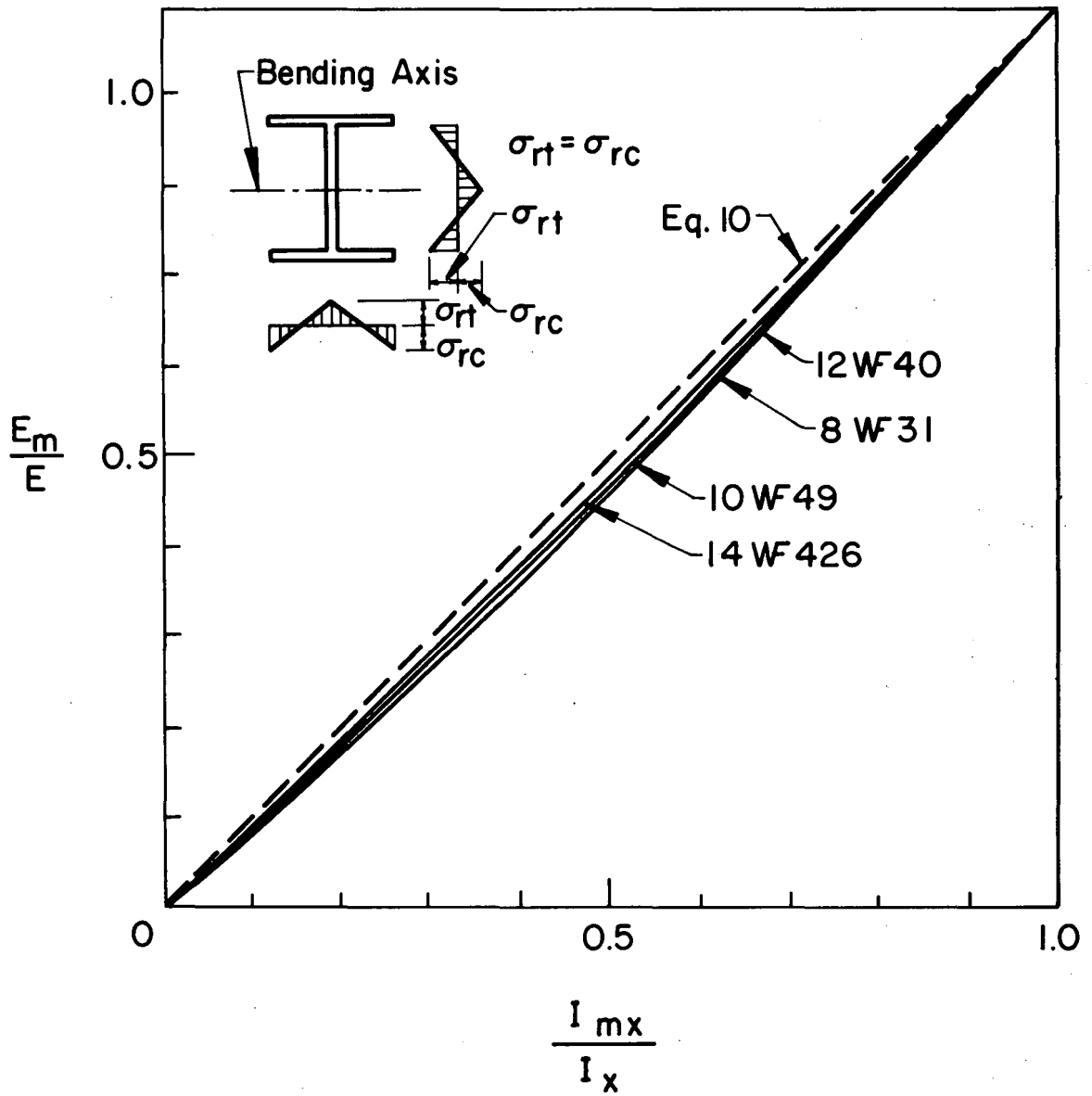


Fig. 5  $\frac{E_m}{E}$  vs.  $\frac{I_{mx}}{I_x}$  Relationship for Rolled WF-Shapes of Mild Steel.

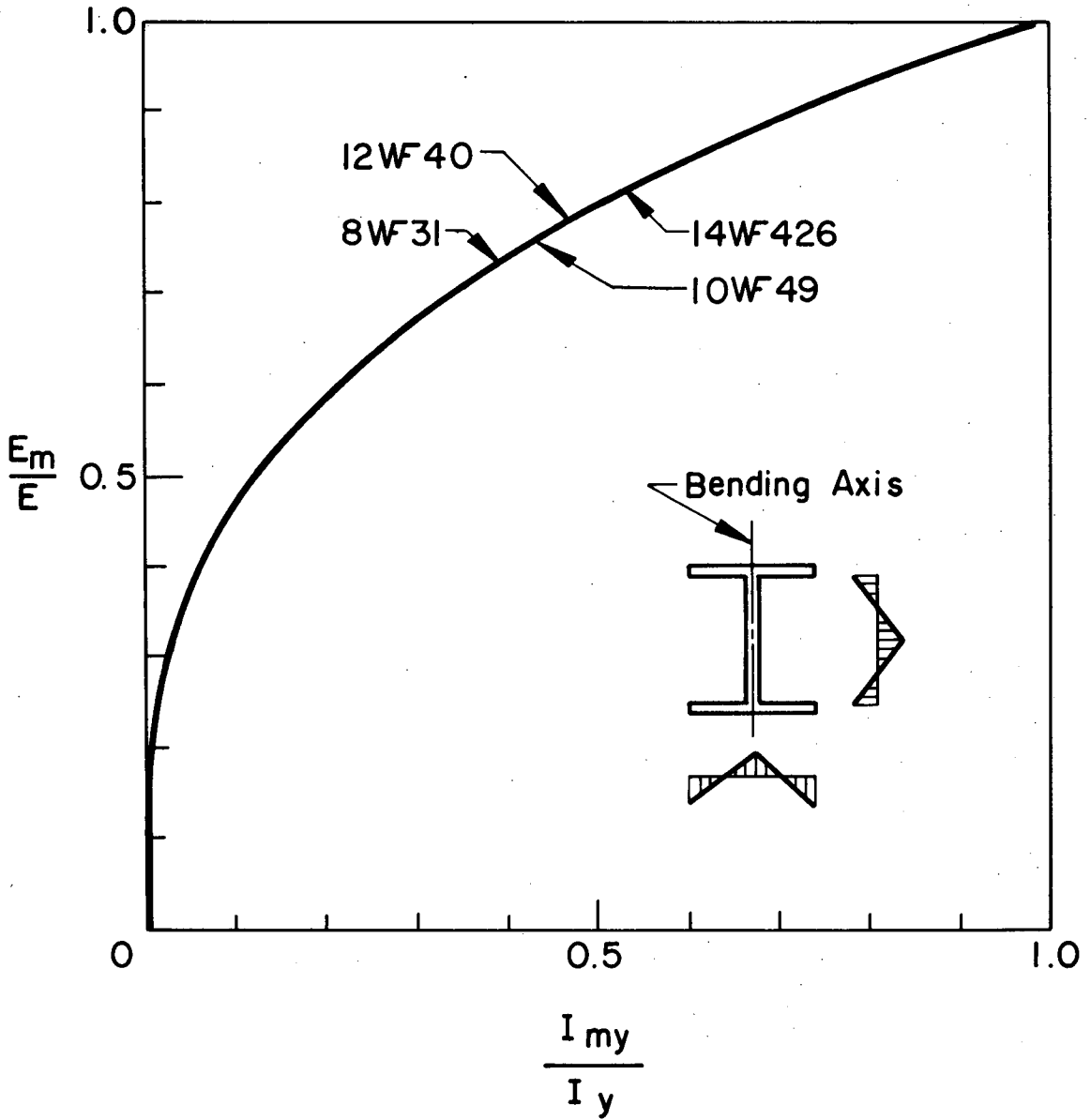
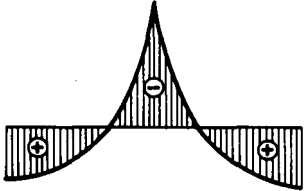
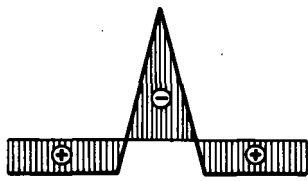
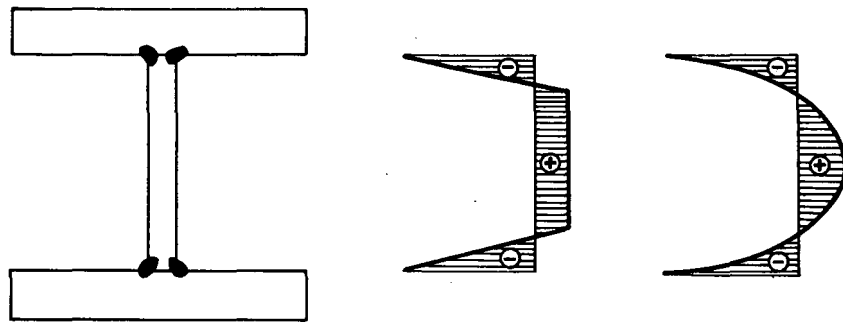


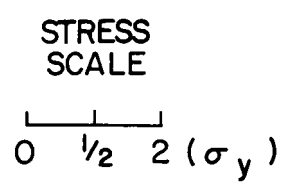
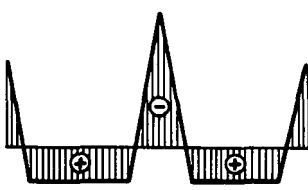
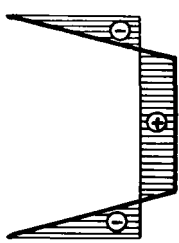
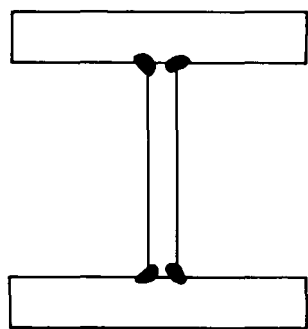
Fig. 6  $\frac{E_m}{E}$  vs.  $\frac{I_{my}}{I_y}$  Relationship for Rolled WF-Shapes of Mild Steel.





- Tension  
+ Compression

WELDED SHAPES WITH UNIVERSAL MILL PLATES



WELDED SHAPES WITH FLAME-CUT PLATES

Fig. 7 Residual Stress in Welded H-Shapes.

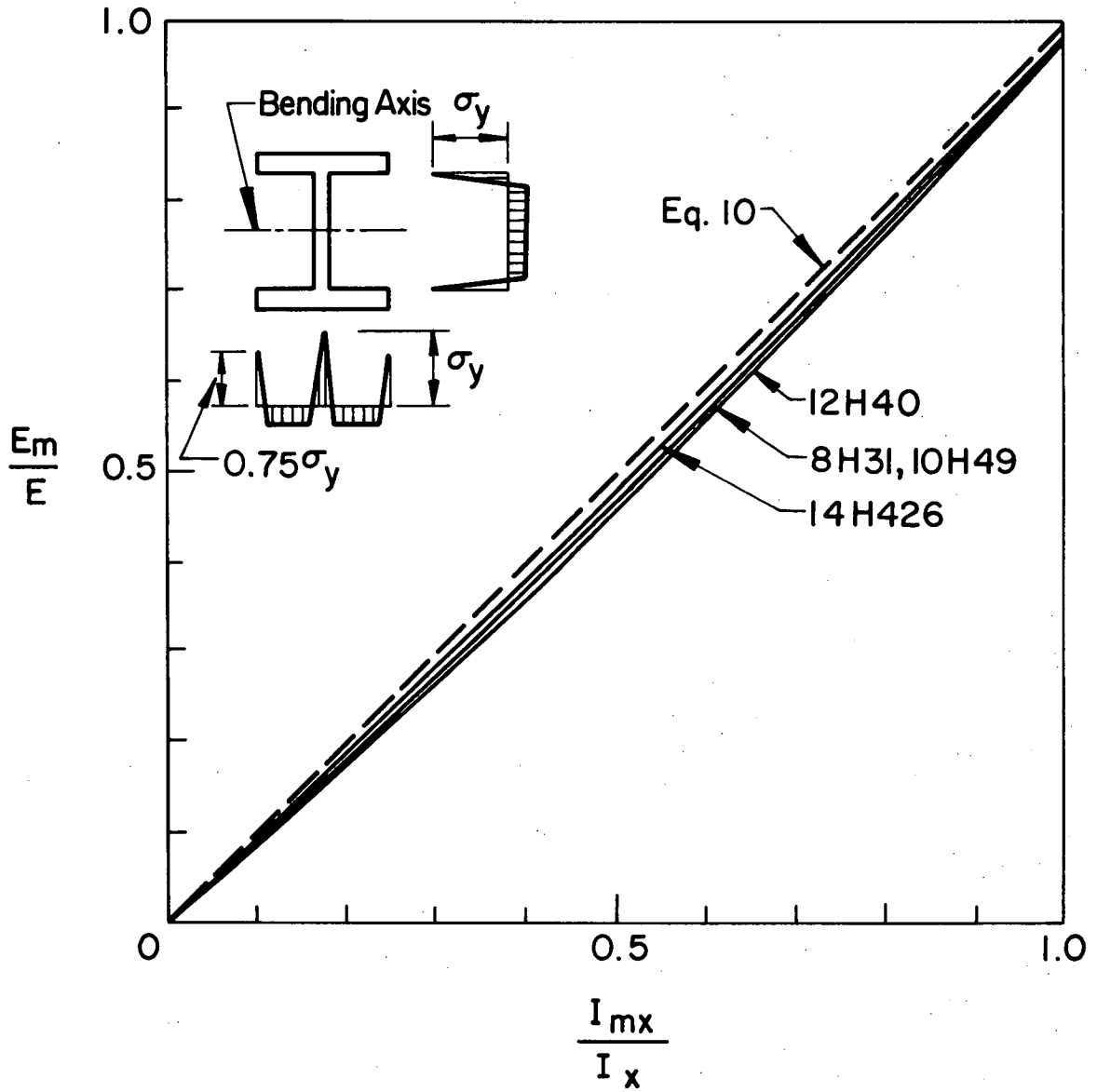


Fig. 8  $\frac{E_m}{E}$  vs.  $\frac{I_{mx}}{I_x}$  Relationship for Welded H-Shapes With Flame-Cut Plates.

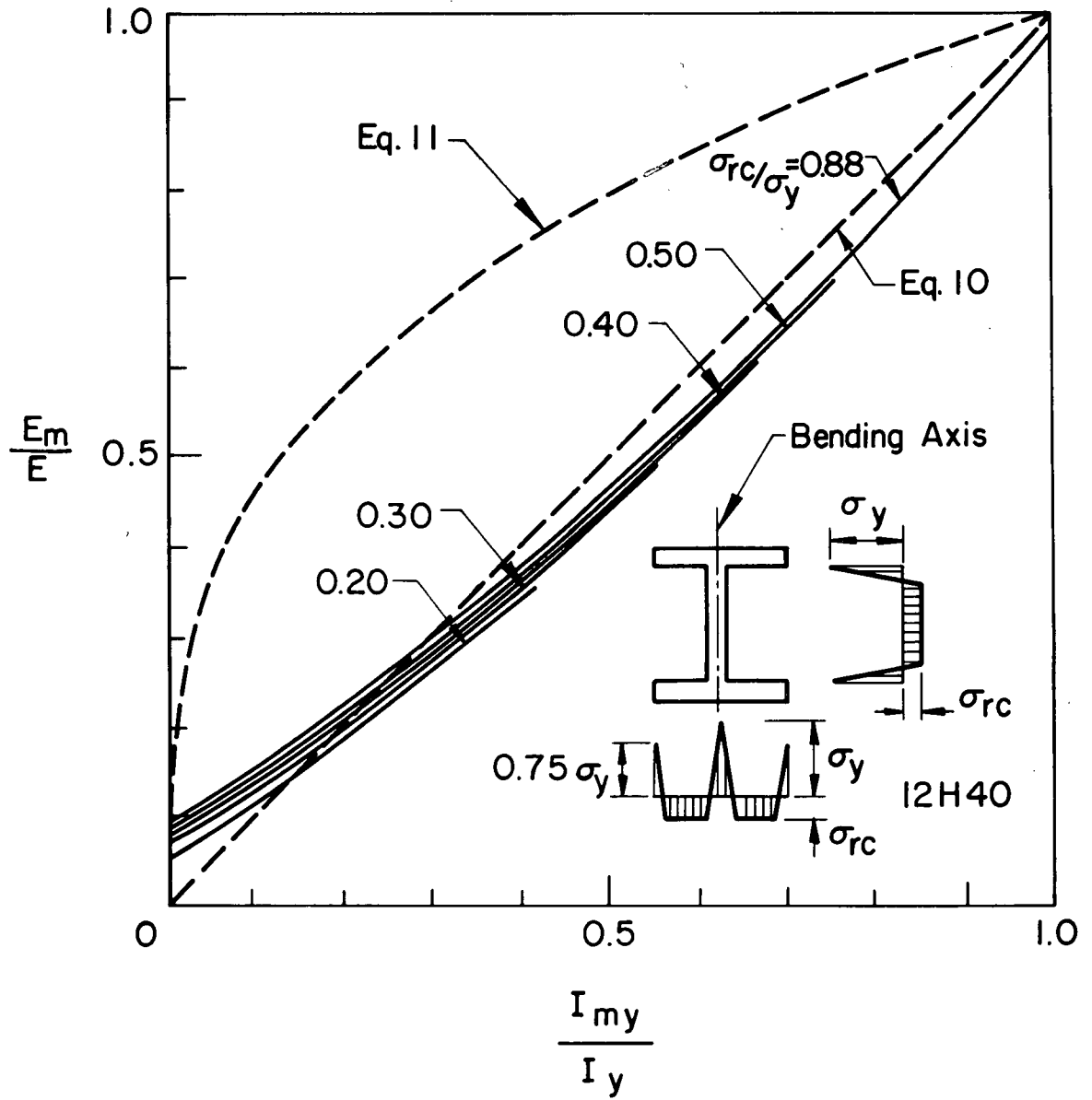


Fig. 9  $\frac{E_m}{E}$  vs.  $\frac{I_{my}}{I_y}$  Relationship for Welded H-Shapes With Flame-Cut Plates.

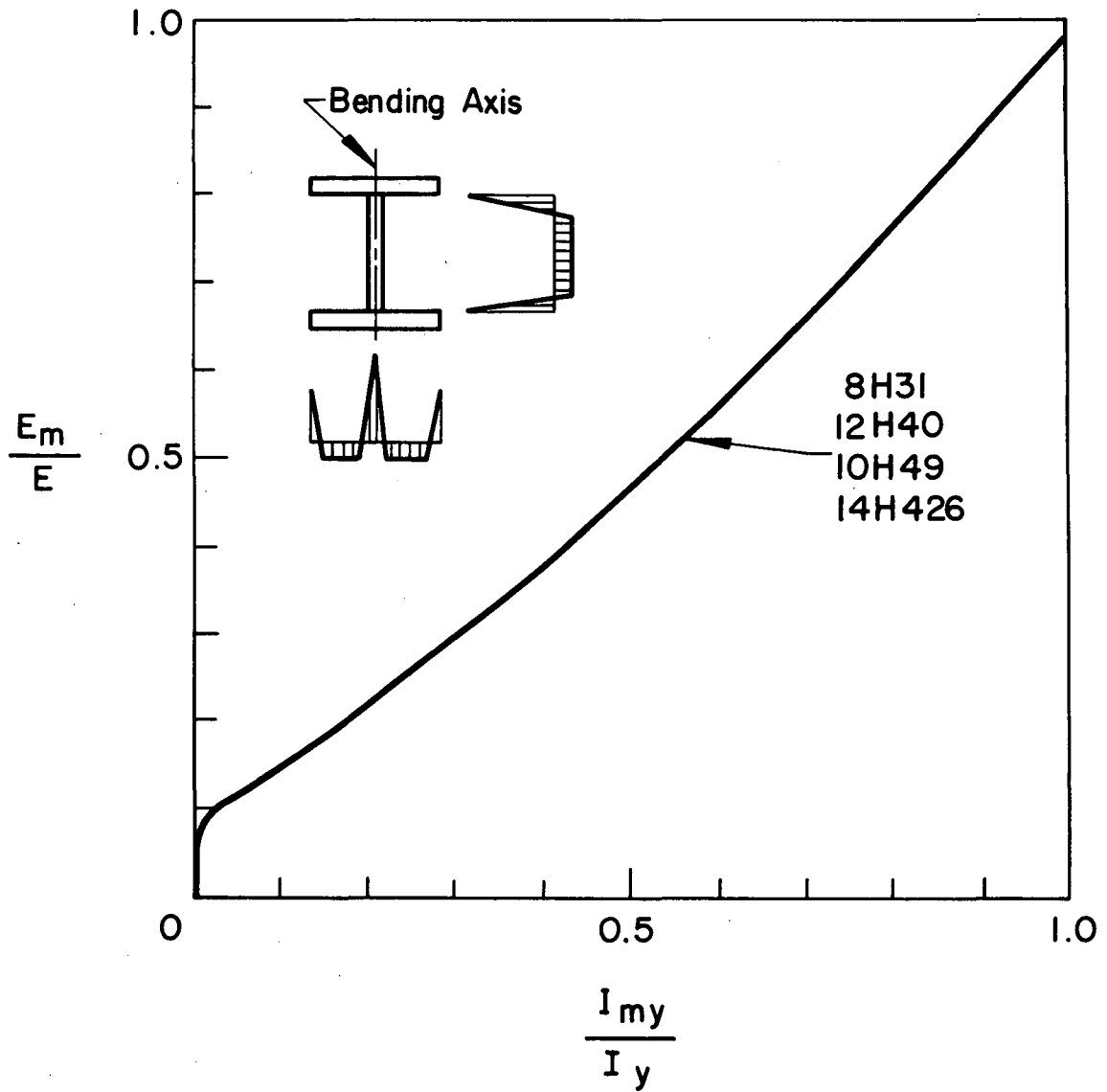
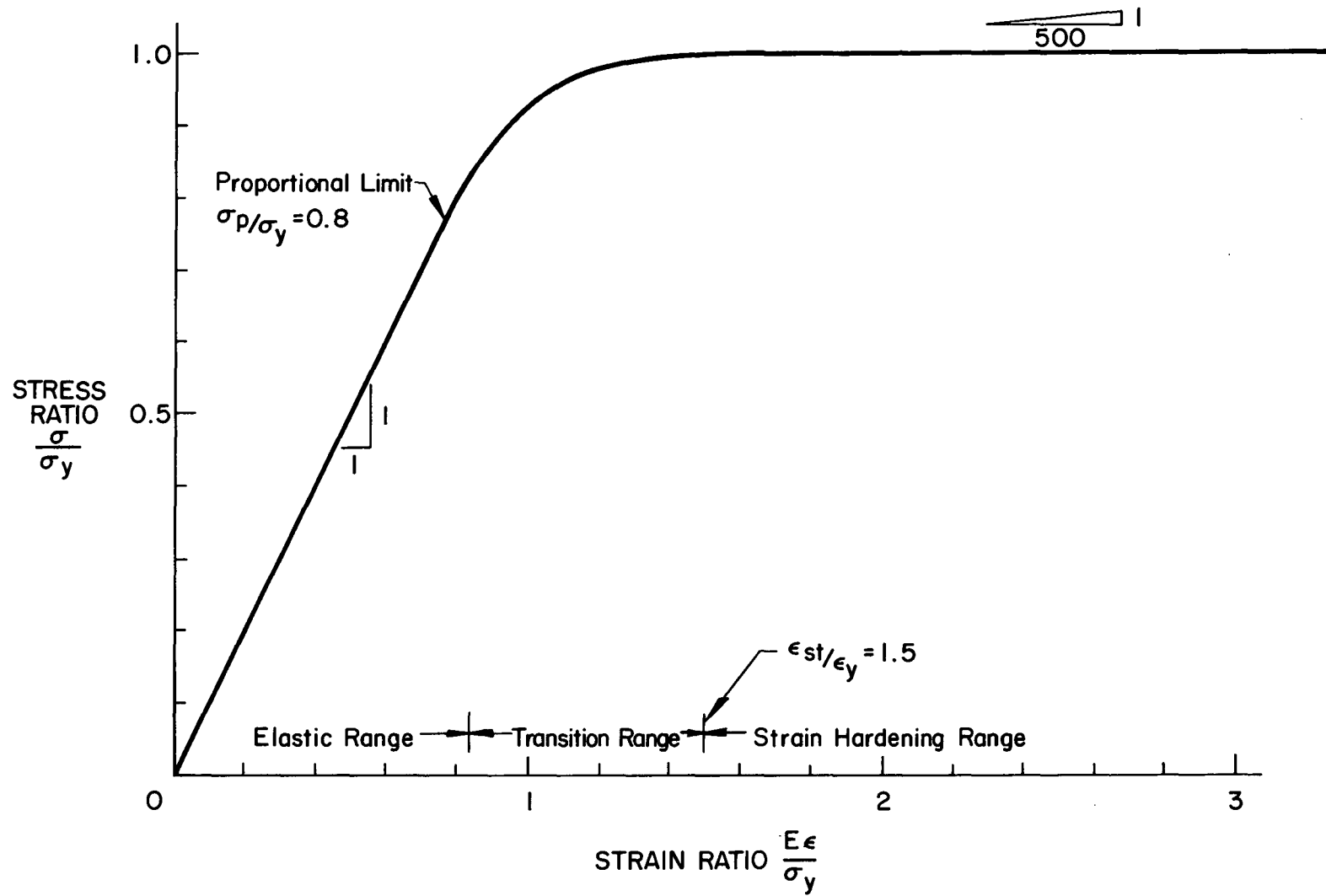


Fig. 10 Suggested  $\frac{E_m}{E}$  vs.  $\frac{I_{my}}{I_y}$  Relationship for Welded H-Shapes With Flame-Cut Plates.



290.18

Fig. 11 Stress-Strain Relationship for A514 Steel.

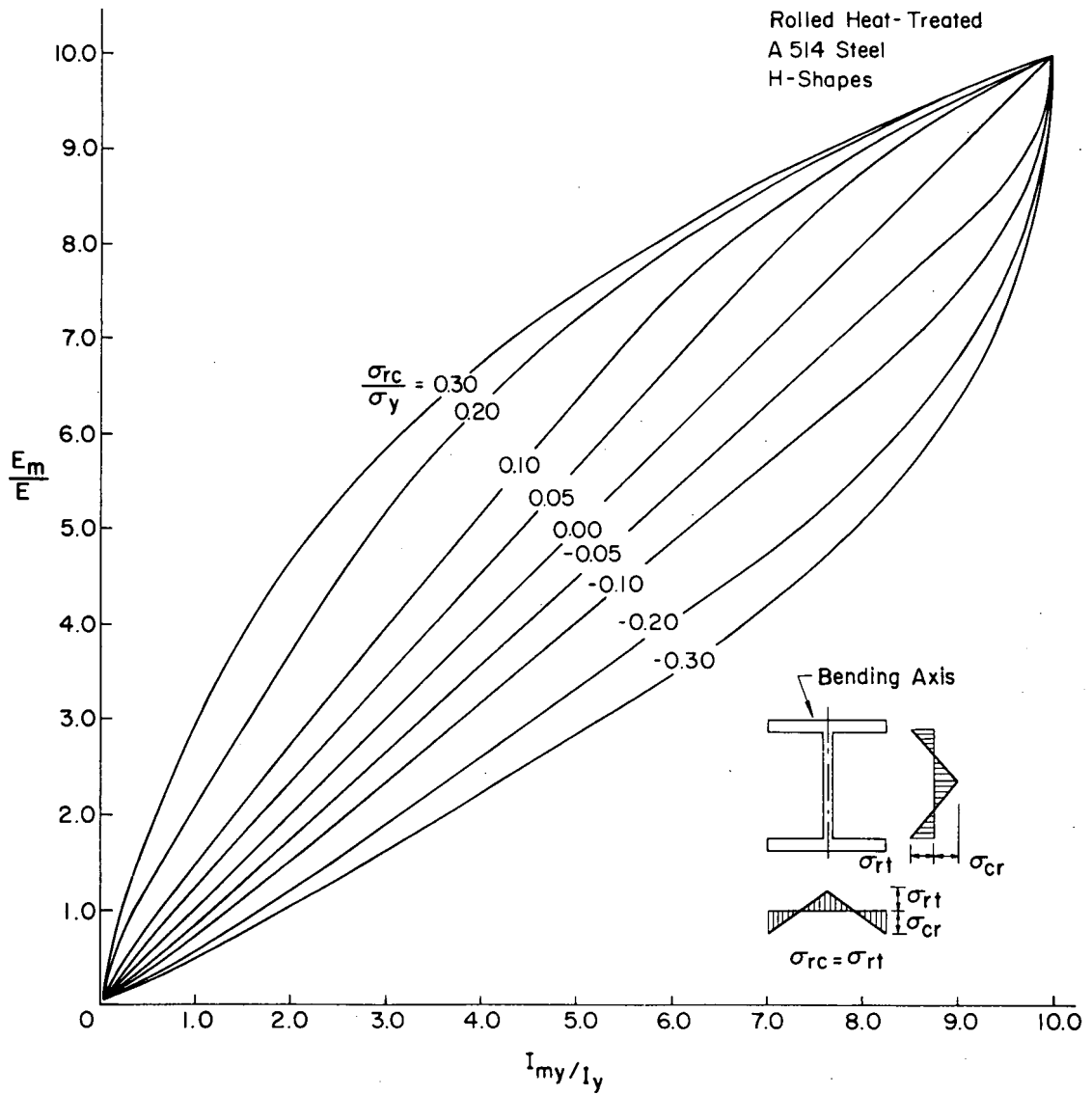


Fig. 12 Effective Modulus vs. Effective Moment of Inertia Relationship.

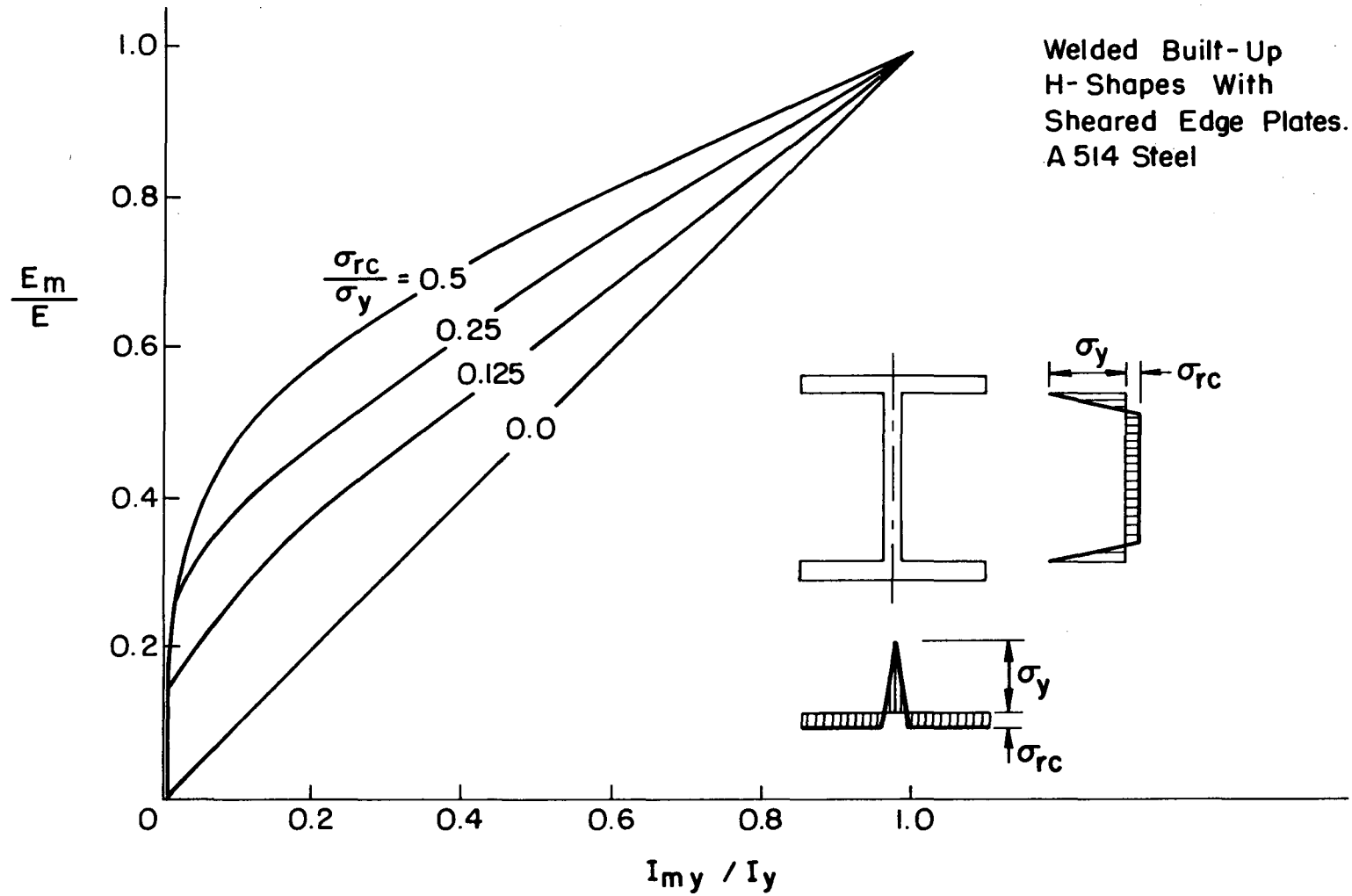


Fig. 13 Effective Modulus vs. Effective Moment of Inertia Relationship.

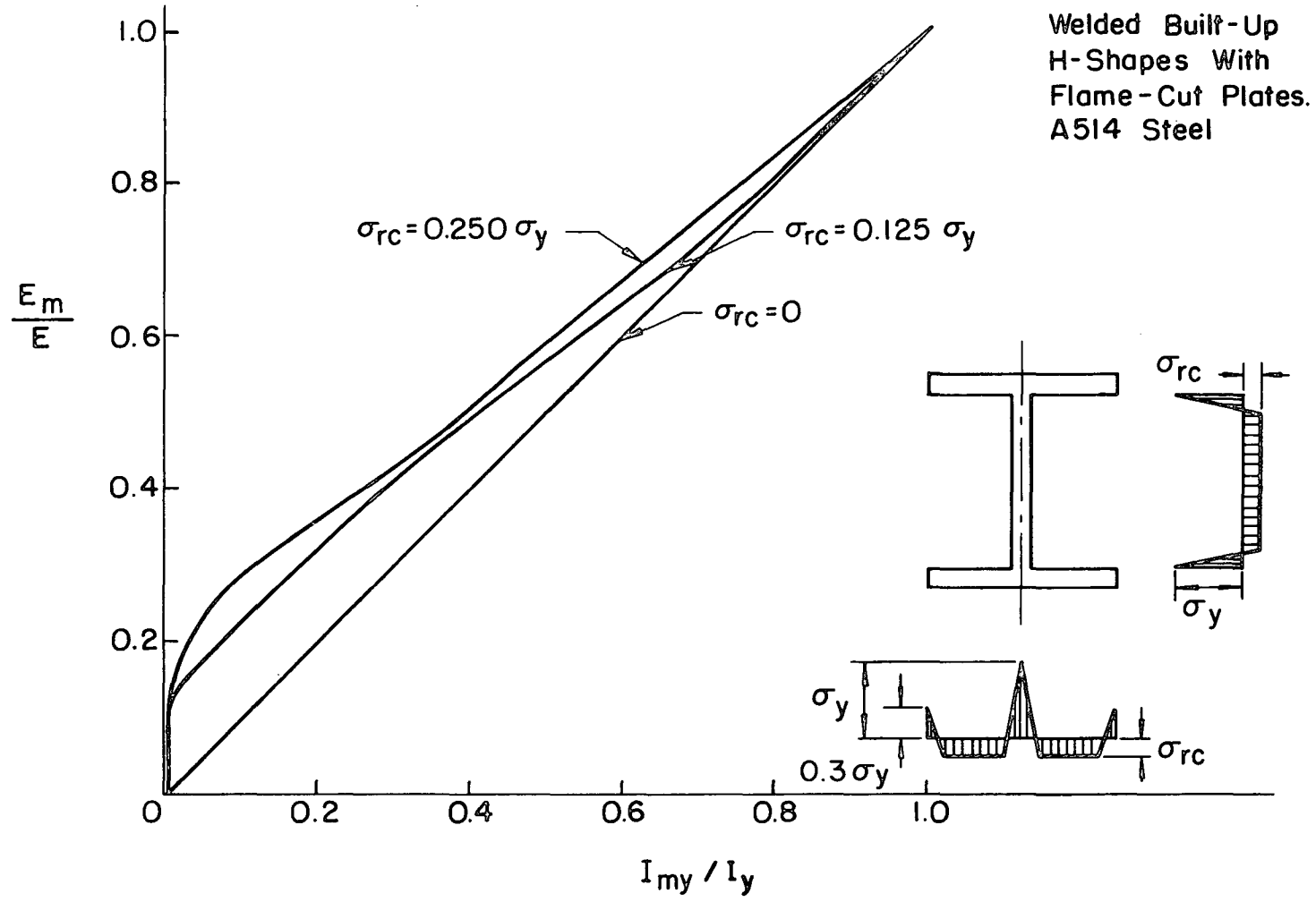
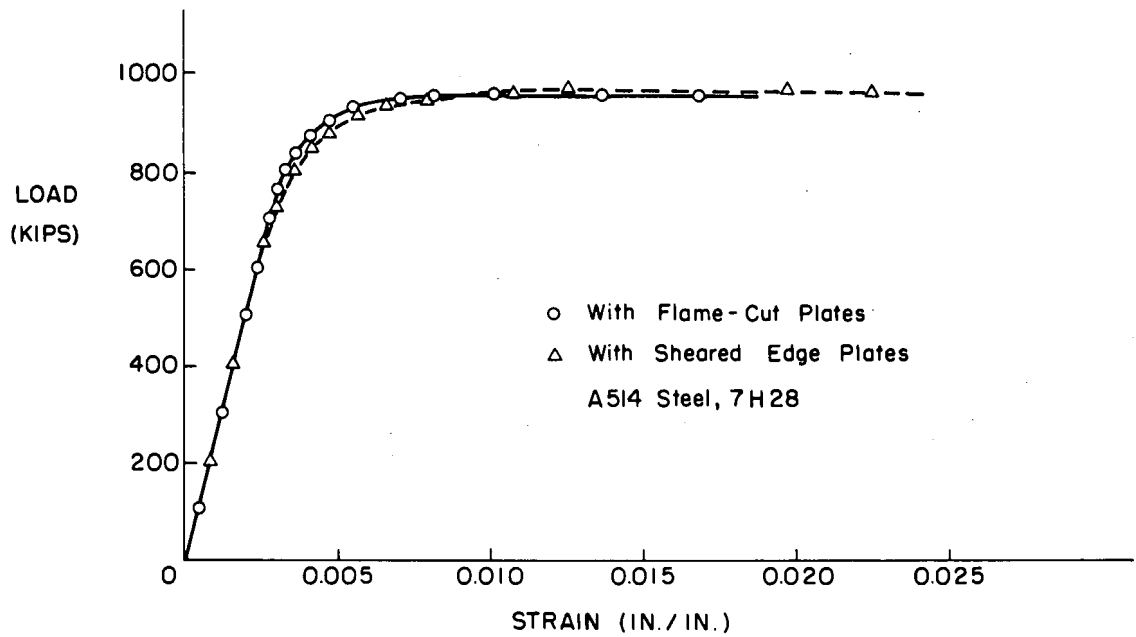
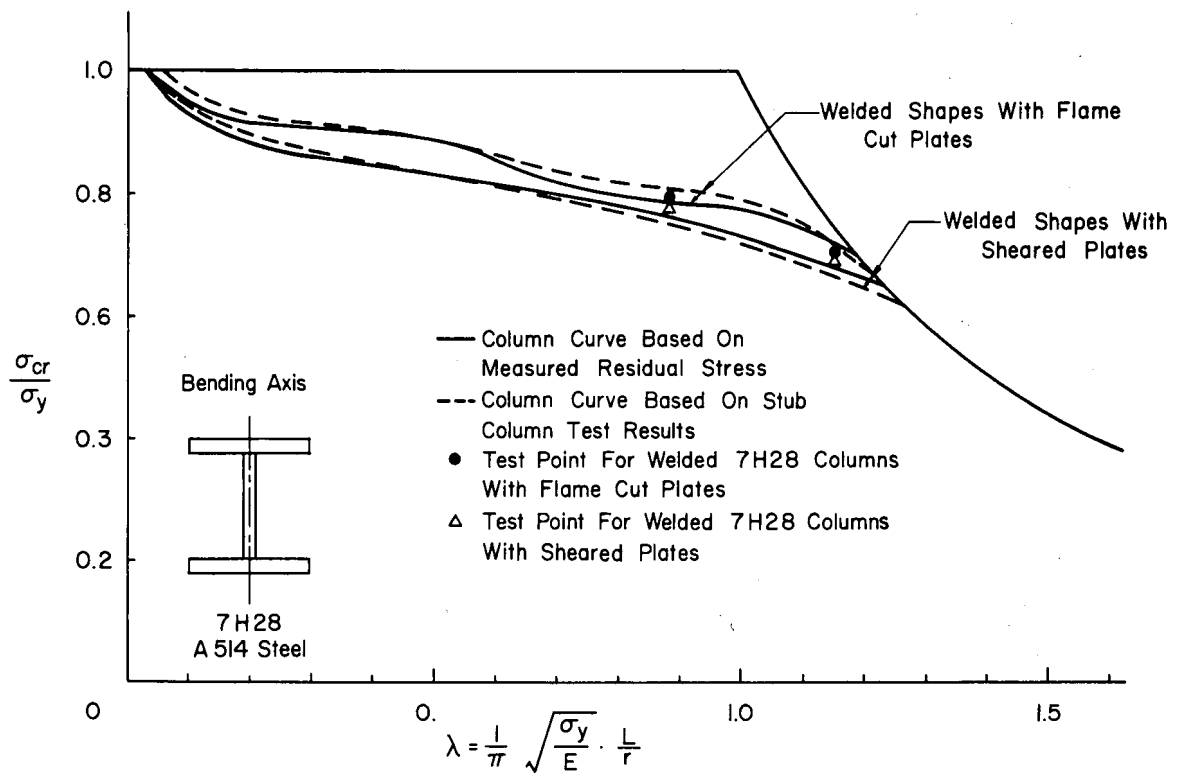


Fig. 14 Effective Modulus vs. Effective Moment of Inertia Relationship.





(a) STUB COLUMN TESTS



(b) COMPARISON OF COLUMN CURVES

Fig. 15 Tangent Modulus Column Curves Based on Stub Column Tests.

10. REFERENCES

1. Johnston, B., Editor  
CRC GUIDE TO DESIGN CRITERIA FOR COMPRESSION  
MEMBERS, Wiley, 2nd edition, 1966.
2. Nishino, F.  
BUCKLING STRENGTH OF COLUMNS AND THEIR COMPONENT  
PLATES, Ph.D. Dissertation, Lehigh University,  
1964. University Microfilms, Inc., Ann Arbor,  
Michigan.
3. Beedle, L. S. and Tall, L.  
BASIC COLUMN STRENGTH, Proceedings, ASCE,  
Vol. 86, No. ST7, July, 1960.
4. Tall, L.  
WELDED BUILT-UP COLUMNS, Ph.D. Dissertation,  
Lehigh University, May, 1961. University  
Microfilms, Inc., Ann Arbor, Michigan.
5. Tall, L.  
STUB COLUMN TEST PROCEDURE, Fritz Engineering  
Report 220A.36, February, 1961; Document.  
C-282-61, class c Document, International  
Institute of Welding, Oslo, June, 1962; CRC  
Tech. Memo No.3, Appendix to "Column Research  
Council Guide" 2nd Edition, Edited by B. G.  
Johnston, Wiley, 1966.
6. Yu, C. K.  
INELASTIC COLUMN WITH RESIDUAL STRESSES,  
Ph.D. Dissertation, Lehigh University, April,  
1968. University Microfilms, Inc., Ann  
Arbor, Michigan.
7. Huber, A. W., and Beedle, L. S.  
RESIDUAL STRESS AND THE COMPRESSIVE STRENGTH  
OF STEEL, Welding Journal, Vol. 33, January, 1954.
8. American Society for Testing and Materials,  
ASTM Standards, Part 3, A370-617, 1961.